

## AN ABSTRACT OF THE PROJECT REPORT OF

Farzana Hasan Shashi for the degree of Master of Science in Electrical & Computer Engineering presented on 02/21/2020.

Title: Design, Fabrication and Characterization of Narrowband Aluminum Plasmonic Grating Filter Array for Spectroscopy in Visible Light Range

Metal grating based plasmonic filters are widely researched for their unique properties of field enhancement and localization of light beyond diffraction limit. However, the plasmonic grating filters reported in literature mostly have broadband outputs making them unsuitable for spectroscopy. In this project, we have designed, fabricated, and characterized an array of 20 plasmonic filters having narrow transmission bands with an average of 17nm FWHM covering the whole visible light range. These filters were fabricated on a single quartz substrate having two thin dielectric layers of Si<sub>3</sub>N<sub>4</sub> and SiO<sub>2</sub> along with aluminum gratings on top. The aluminum gratings for all 20 filters were patterned using a single step focused ion beam etching making the fabrication process time and cost effective. The filters were characterized using a fiber-based testing setup and later used for high-fidelity signal reconstruction integrating the device with a CMOS imager.

©Copyright by Farzana Hasan Shashi  
02/21/2020  
All Rights Reserved

Design, Fabrication and Characterization of Narrowband Aluminum Plasmonic  
Grating Filter Array for Spectroscopy in Visible Light Range

by  
Farzana Hasan Shashi

A PROJECT REPORT

submitted to

Oregon State University

in partial fulfillment of  
the requirements for the  
degree of

Master of Science

Presented 02/21/2020  
Commencement June (2020)

## ACKNOWLEDGEMENTS

I would like to express my sincere gratitude to my supervisor Dr. Alan Wang, for guiding me throughout my research project. He has helped me develop the correct approach to problem solving as well as research methodology. I have been able to complete this project successfully due to his unwavering patience and prudent advices. I would also like to thank my committee members, Dr. Li-Jing Cheng and Dr. Matthew Johnston for their time and effort in supporting me. My heartfelt thanks and appreciation to Dr. Glencora Borradaile, without her support I would not be able to reach the point to present my research.

I am grateful to have wonderful lab mates, who have helped me learn and supported me with resources along every step of the way. I hope this tradition of a supportive work-environment in our lab keeps going strong, and I wish my lab mates all the success in their academic and professional lives.

Lastly, I would like to thank my parents, they have given all their lives to help me reach where I am today. Without their firm belief in me, I would not be able to come so far. My parents are my strength, and I would try my best to make them proud through my work.

## CONTRIBUTION OF AUTHORS

Jyotindra R. Shakya (PhD Candidate, Dept. of ECE, Oregon State University) has major contribution in developing the design of the device, specifically demonstrating that Aluminum is the best choice for the metal grating layer. I would also like to acknowledge him for assisting me throughout the fabrication process of the device.

## TABLE OF CONTENTS

	<u>Page</u>
1 Introduction.....	1
1.1 Plasmonics.....	1
1.2 Extraordinary Optical Transmission.....	2
1.3 Plasmonic Filters for Spectroscopy.....	3
2 Literature Review.....	4
3 Materials and Methods.....	5
3.1 Device Design Simulation.....	5
3.2 Device Fabrication.....	8
3.2.1 Substrate Preparation.....	8
3.2.2 Focused Ion Beam Etching.....	9
3.3 Testing Setup.....	11
4 Results and Discussion.....	14
4.1 Data Processing.....	14
4.2 Filter Characterization.....	14
4.3 Future Application.....	15
5 Conclusion.....	15
Bibliography.....	16

## LIST OF FIGURES

<u>Figure</u>	<u>Page</u>
1. 3D Schematic of the Plasmonic Filter.....	5
2. Shift of Transmission Peak as a Function of Period P.....	6
3. Simulated Transmission Spectra of 20 filters (Period 260nm-450nm).....	7
4. Field Distribution in the Device.....	8
5. SEM Image of the Evaporated Aluminum Layer.....	9
6. Magnified Images of the Metal Gratings.....	10
7a. Top View of the 5x4 Filters Array.....	11
7b. Optical Image of the Filter Array.....	11
8. Testing Setup Schematic for Filter Characterization.....	12
9. Testing Setup Built for Filter Characterization.....	13
10. Measured Transmission Spectra of the filter Array.....	14

## LIST OF TABLES

<u>Table</u>	<u>Page</u>
2.1 Literature Review.....	4
3.1 Quanta 3D Writing Conditions Used.....	10



## 1 Introduction:

### 1.1 Plasmonics

The pursuit of going beyond the fundamental problem of optical diffraction limit has led science to the exciting new field of Plasmonics. The integrated electronics technology is rapidly reaching its speed and bandwidth limitations, and this has compelled the scientists to consider replacing electronic signals with light signals as information carriers as the solution leading to the field of photonics. However, photonic devices and integrated circuits comes with very low scopes of integration and miniaturization owing to the diffraction limit of light in dielectric media, which does not allow the condensation of electromagnetic waves into regions smaller than the wavelength of light in the material [1]. Plasmonics is the area of nanophotonics that study the conversion of optical signals into intense, engineered, localized field distributions or coupling of light to deep-subwavelength guided modes using metallic nanostructures [2]. The key element of Plasmonics, surface plasmons are defined as the quanta of collective electronic excitation on good metal surfaces. When the phase velocity of surface plasmon is comparable to the velocity of light (in retarded field), surface plasmon can couple with the free electromagnetic field. The quanta of this combined excitation is called surface plasmon polartion (SPP) and it propagates along the metal surface. However, light incident on an ideal surface cannot couple with the surface plasmons to excite SPPs. The way to excite SPPs are either through prism coupling or grating coupling [3]. The electromagnetic field of a SPP is confined to the near vicinity of the dielectric–metal interface which leads to an enhancement of the electromagnetic field at the interface, resulting in an extraordinary sensitivity of SPPs to surface conditions [4]. Due to this property, a variation the

period of gratings used to couple the light will lead to a variation in the peak wavelength of the excited SPP modes. Exploiting this property, plasmonic devices can be used for wavelength filtering and spectroscopy.

## 1.2 Extraordinary Optical Transmission

From classical aperture theory, we can say that the amount of light transmitted through an aperture in an opaque metal film is proportional to the aperture area. The transmittance ( $T$ ) is given by  $T \propto (d/\lambda)^4$  when  $\lambda > d$ , where  $d$  is the aperture diameter and  $\lambda$  is the wavelength of the transmitted light [5]. It was found later that the amount of transmitted light at certain wavelengths was much larger than calculated by the classical aperture theory and the material seemed more transparent than it should be at certain wavelengths. This phenomenon was named extraordinary optical transmission (EOT). It was suggested that EOT was due to the excitation of surface plasmon resonances through grating coupling [6], since the loss in SPP modes is a function of wavelength [1]. The important finding was that the peaks of maximum transmission were related to periodicity of the apertures. Hence it is possible to tune the wavelength of the maximum transmission by tuning the periodicity of the apertures leading to possible application in wavelength filtering and potentially spectroscopy. For periodic metallic nanostructures, at normal incidence, the wavelength of SPP resonance ( $\lambda_{SP}$ ) from an array of nano-apertures with square lattice symmetry can be estimated using the periodicity of the array and the dielectric constants of the adjacent medium and the metal [7].

### 1.3 Plasmonic Filters for Spectroscopy

Spectroscopy is the technique of separating an electromagnetic signal into its spectral components. Traditional spectrometers in visible-light range based on diffraction gratings are bulky. Due to ever-growing use of optical spectroscopy in including but not limited to biomedical, industrial, military, life sciences, and other surveillance applications, there is need for compact on-chip spectrometers that are also cost-effective. Exploiting the optimization of extraordinary optical transmission using plasmonic metal gratings resulting in selective wavelength filtering makes plasmonic devices suitable for spectroscopy [8]. The transmission properties of plasmonic metal filters consisting of periodic grating arrays are mainly controlled by the design of their physical structure. That is by tuning the aperture size, shape, and periodicity, the transmission spectra of the array can be tuned with only a single thin metal layer. Hence, plasmonic color filters are very cost effective as well as can be made compact for spectroscopic applications. Other advantages of plasmonic filters over conventional filters, include higher reliability under exposure to high temperature and humidity [9].

In this project, an array of 20 filters were fabricated on a single device. Each filter had a periodicity that corresponded to a peak transmission wavelength, thus 20 filters covering the whole visible light range of 400nm to 700nm wavelength with a target Full Width Half Maximum (FWHM) of 15nm. The filters were characterized using conventional spectrometer and a fiber based testing setup, however, combination of such an filter array with a CMOS imager with proper calibration will be potentially applicable in a compact on-chip signal reconstruction system eliminating the need of such bulky spectrometers and testing setups.

## 2 Literature Review:

Plasmonic filters with different structures targeting different regions of the electromagnetic spectrum have already been reported in literature. However, these reported filter designs have wide FWHMs. Although these filters are suitable for different broadband image sensors and display technologies, they are not narrow-band enough for spectroscopic applications. A comprehensive account of the various plasmonic filter designs and their applications found in literature are summarized below.

	Device Structure	Application
[10]	Glass/Si <sub>3</sub> N <sub>4</sub> /SiO <sub>2</sub> /Ag grating	Broadband output with FWHM = 30nm
[11]	Ag/SiO <sub>2</sub> /Ag cavity	Broadband output with FWHM = 40nm
[12]	Ag vertical nanorod array	Broadband output for color generation
[13]	Al nanorod array	Broadband output for display technology
[14]	Al nanohole array on Si/Si <sub>3</sub> N <sub>4</sub> /SiO <sub>2</sub>	Broadband output for RGB imaging
[15]	Quartz/Au/LC/PI/ITO	Broadband output for RGB imaging
[16]	SiN <sub>x</sub> /SiO <sub>2</sub> /Al nanostructure/SiO <sub>2</sub>	Broadband output for RGB imaging
[17]	Glass/Al triangular-lattice hole arrays	Broadband RGB Filters
[18]	Glass/Al equilateral triangular and circular shaped hole arrays	Broadband output for RGB imaging
[19]	Glass/MgF <sub>2</sub> /Al/ZnSe	Color Filters for LCD display

Table 2.1: Literature Review

### 3 Methods and Materials:

#### 3.1 Device Design Simulation

The device structure, as shown in Figure 1, consists of two thin dielectrics layers deposited on top of a Quartz substrate. We are denoting the top dielectric layer of SiO<sub>2</sub> as the buffer layer with a thickness of  $T_B$ , and the layer of Si<sub>3</sub>N<sub>4</sub> between the buffer layer and the quartz substrate as the waveguide layer with a thickness of  $T_{WG}$ . The substrate has a thickness of 0.5mm. We have chosen Aluminum as the metal layer for grating coupling of the light signal due to its excellent plasmonic properties in visible light range especially low loss as well as for the low-cost established processing techniques compatible with CMOS technology [20]. The metal layer has a thickness of  $T_M$ , and it has a periodic grating structure with a period  $P$  and a gap  $G$  between the gratings. The optical transmission properties of the structure were simulated using RSoft (DiffractMOD) software from Synopsys, which uses Rigorous Coupled Wave Analysis (RCWA) technique. RCWA approach is used to analyze the diffraction caused by general planar gratings bounded by two different media [21]. We only consider transverse-magnetic mode for this simulation.

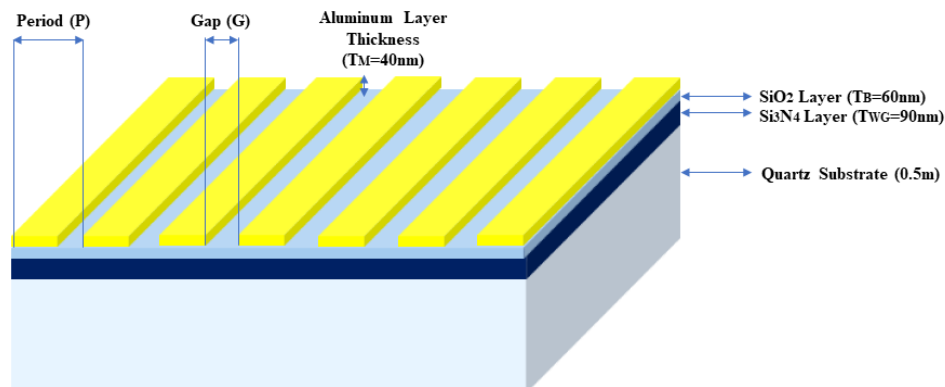


Figure 1: 3D Schematic of the Plasmonic Filter

The three dielectric layers including the quartz substrate form a waveguide for the specific frequency band coupled in [10]. The device was simulated with various combination of TWG, TB, TM, as well as P and G to figure out how each parameter affects the transmission. The period P controls the peak transmission wavelength due to EOT effect as stated earlier. The thicknesses of the buffer layer and the waveguide layer as well as their ratio are associated with the coupling of light and hence have effect on the FWHM of the transmission peak. The gap G also effects the FWHM as well as the field enhancement. In this project, we have selected TWG = 90 nm, TB = 60 nm, TM = 40 nm, G = 40 nm as the final parameter values and used them for all the simulations presented in the report and the device fabrication. The period P was varied from 260nm to 450nm with a step of 10nm for the 20 filters simulated and fabricated. The variation of the transmission peak as function of period is shown in figure 2.

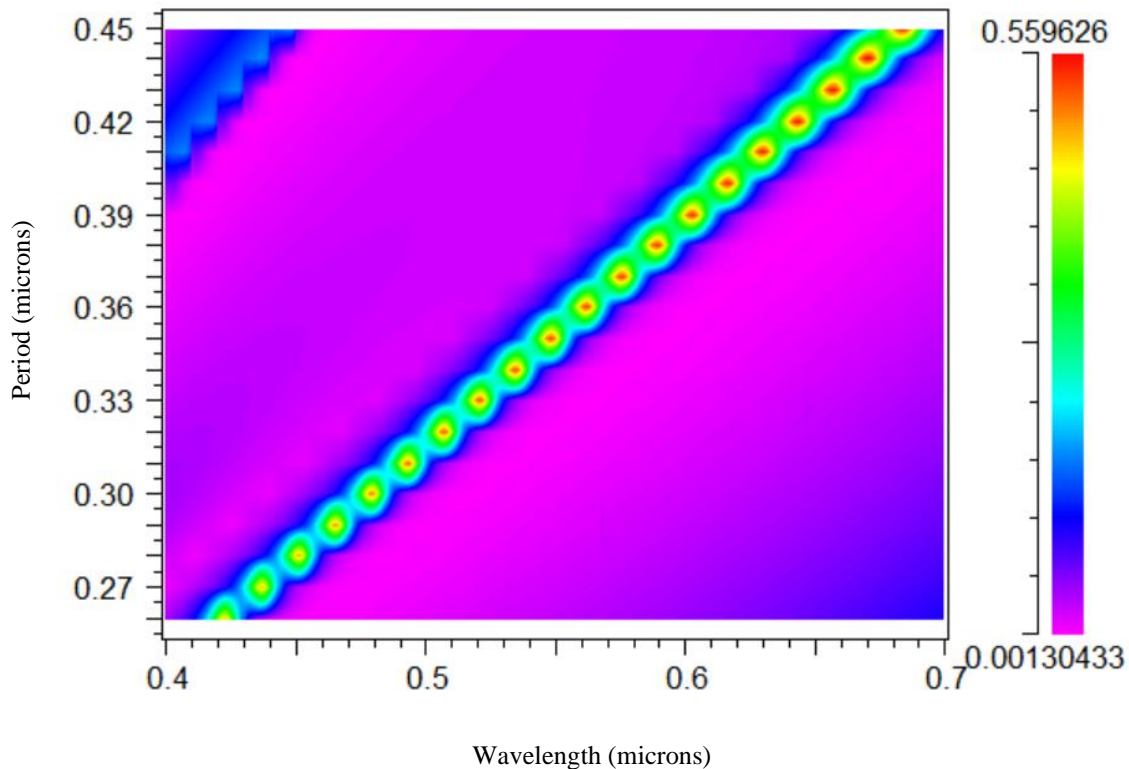


Figure 2: Shift of Transmission Peak as a Function of Period P

The resolution for the output spectrum was chosen 1nm in RSoft. The simulation was done for 1-dimensional grating and the launched field was normal to the substrate. Figure 3 shows normalized transmission spectra for all 20 simulated filters.

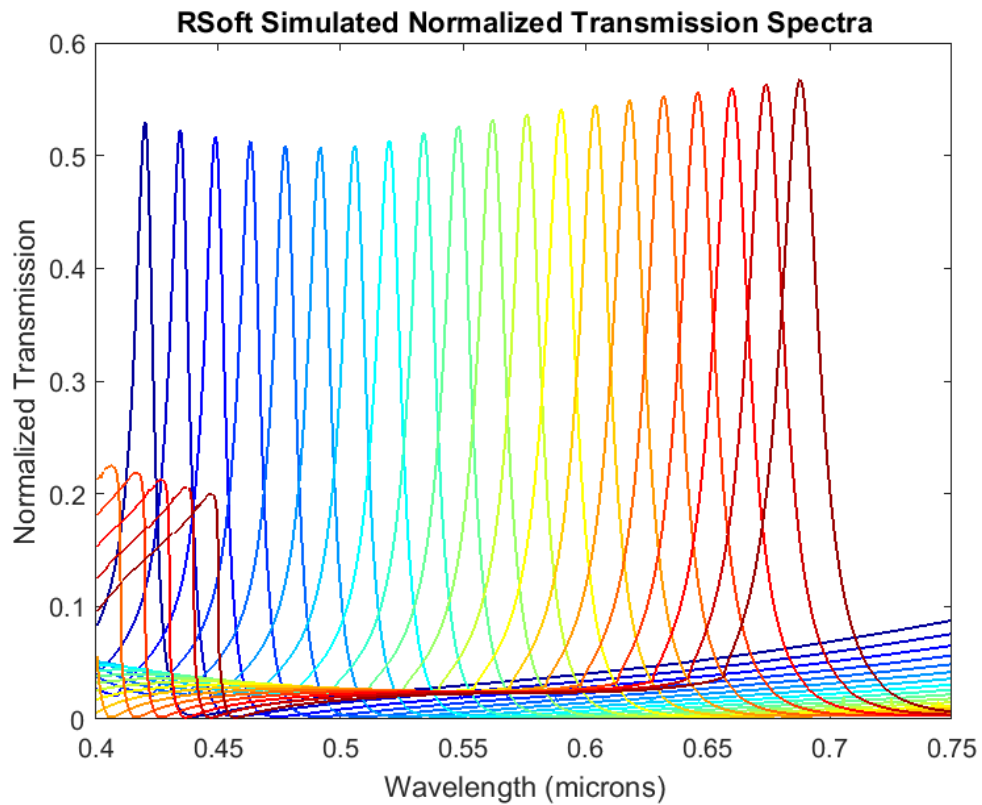


Figure 3: Simulated Transmission Spectra of 20 filters (Period 260nm-450nm)

Figure 4 shows the field distribution in the device along transmission axis for a filter with a period of 350 nm at its maximum transmission peak wavelength of 535 nm. It shows a field enhancement factor of 5 inside the buffer layer.

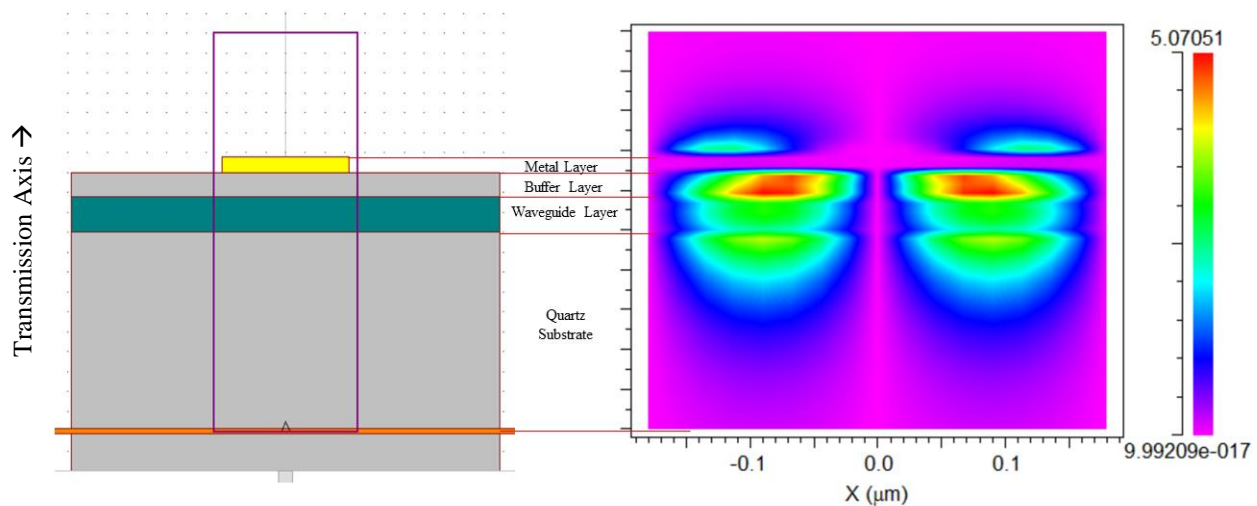


Figure 4: Field Distribution in the Device

## 3.2 Device Fabrication

### 3.2.1 Substrate Preparation

We started with a polished quartz substrate (4" diameter, 0.5mm thickness) with 90 nm of  $\text{Si}_3\text{N}_4$  layer deposited through plasma-enhanced chemical vapor deposition (PECVD) process as the waveguide layer and 60 nm of  $\text{SiO}_2$  deposited on top of the waveguide layer through the same PECVD process as the buffer layer. The wafer was diced into 1" by 1" substrates using wafer saw. The substrate was cleaned using Acetone – Isopropanol Alcohol – Deionized water in that order and then using oxygen plasma for 1minute before metal deposition. 40 nm layer of aluminum was thermally evaporated on the top of the buffer layer of a substrate using the Veeco 7700 series thermal evaporator. The aluminum layer was deposited at a rate of 0.01nm/s to ensure a smooth



surface without porosity [20]. Figure 5 shows the Scanning Electron Microscope (SEM) image of the evaporate Aluminum surface.

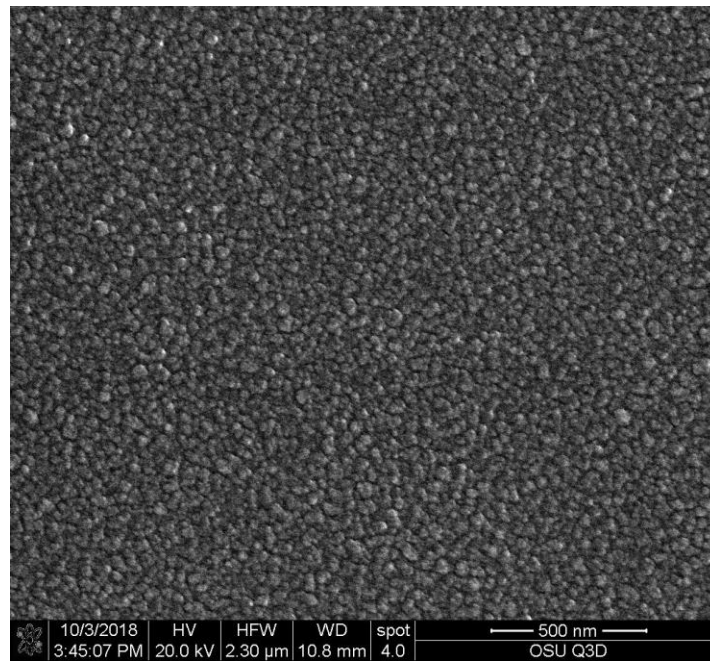


Figure 5: SEM Image of the Evaporated Aluminum Layer

### 3.2.2 Focused Ion Beam Etching

The grating patterns for all 20 filters was designed using AutoCAD and transferred to the NPGS software system for conversion to make them compatible with the FEI Quanta 3D Dual Beam Electron Microscope which was used to pattern the aluminum layer using focused ion beam (FIB) etching technique. An 5x4 array of 20 filters were patterned varying the periodicity from 260-450 nm in a single step. Each filter is  $25\mu\text{m}\times 25\mu\text{m}$  in size, and the center to center distance between

the filters is 50  $\mu\text{m}$ . The aluminum layer was milled using 30keV Ga<sup>+</sup> ions at 30pA current with dose of 35 mC/cm<sup>2</sup>. The required dose was optimized for the minimum write-time while maintaining the precision of the features. The average write time was 15 minutes per filter.

Figure 6 shows the magnified SEM images of etched metal gratings for the filter with 450nm period.

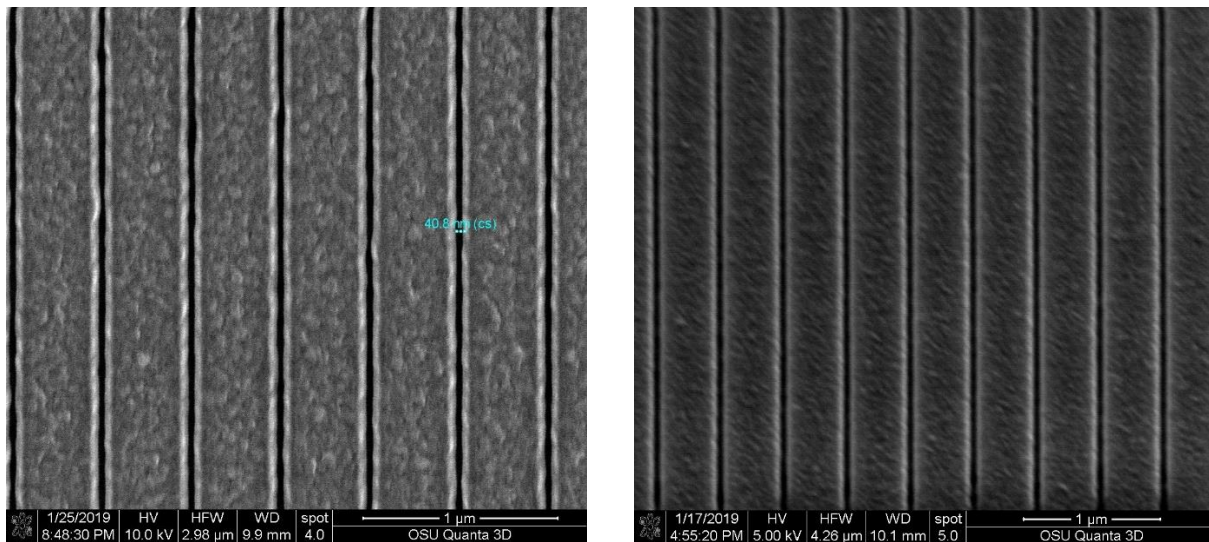


Figure 6: Magnified Images of the Metal Gratings

Other conditions used in the Quanta 3D for the patterning are summarized below in Table 3.1.

Writing Mode	“Continuous”	Center to Center Distance	5
Magnification	2000	Line Spacing	5

Table 3.1: Quanta 3D Writing Conditions Used

Figure 7(a) shows the SEM top view of the 5x4 array of filters and Figure 7(b) shows the optical image of the filter array using polarized light taken with Leica DM 5000-D Computerized Optical Microscope.

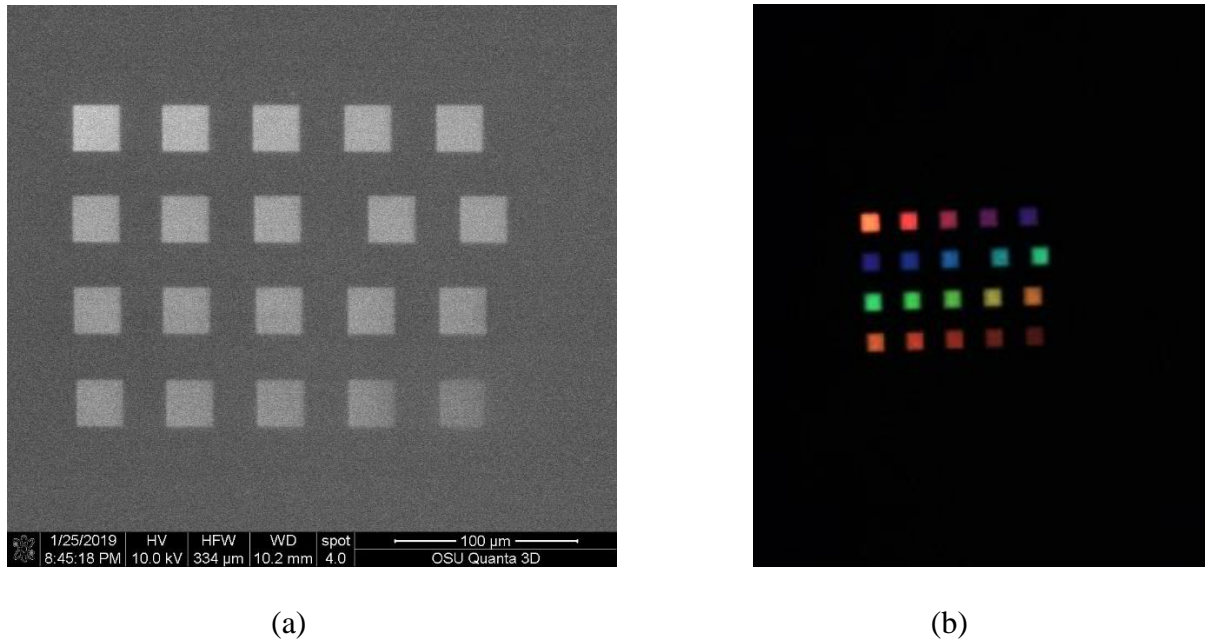


Figure 7: (a) Top View of the 5x4 Filters Array, (b) Optical Image of the Filter Array

### 3.3 Testing Setup

A simple fiber-based testing setup was built to characterize the filters. A super-K compact supercontinuum light source (NKT Photonics, Denmark) was used as a broadband input. The output light from the light source was collimated and normally incident onto the substrate from the Quartz side after passing through a polarizer. The sample device was mounted on a xyz - translational stage. A multimode optical fiber with a core of 62.5 micron was used to collect the

light from the filters. A portable microscope with 20x objective lens was used to couple the light from a filter to the optical fiber. The sample was moved manually in x, y, and z direction using the stage knobs to couple the light efficiently with the fiber. The output light from the other end of the multimode fiber was coupled into the input fiber end of the Ocean Optics USB2000+ spectrometer and the data were collected using Oceanview Spectroscopy software. The data were averaged over 10 readings. Figure 8 shows the schematics of the testing setup and Figure 9 shows the real testing setup.

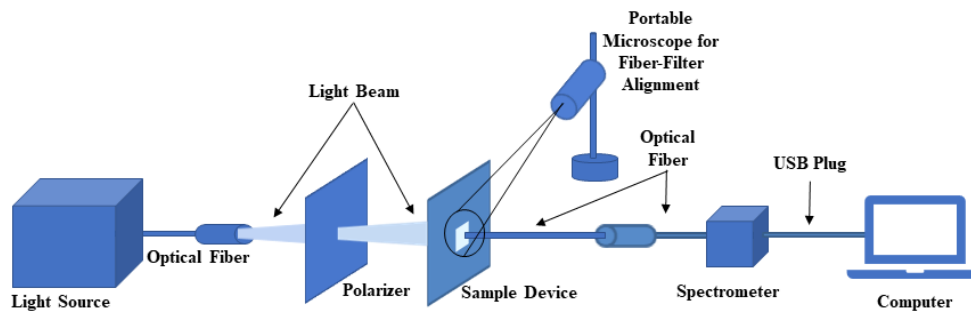


Figure 8: Testing Setup Schematic for Filter Characterization

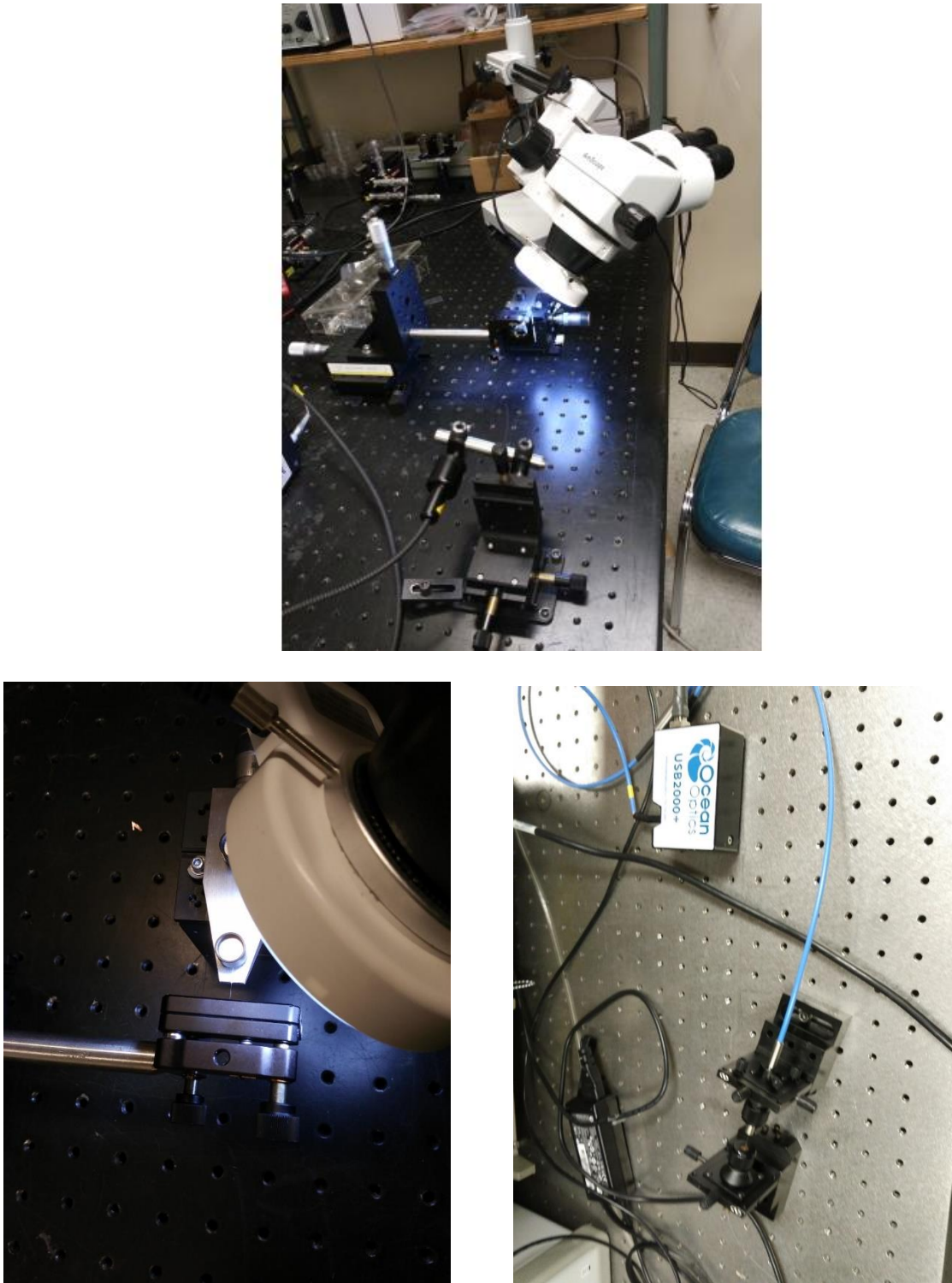


Figure 9: Testing Setup Built for Filter Characterization

## 4 Results

### 4.1 Data Processing

The source was directly measured, and the filter outputs were normalized to the source signal. Since the fiber core is larger than the filter size, transmission from the aluminum layer without any grating was recorded and subtracted from the filter output for background calibration.

### 4.2 Filter Characterization

Figure 10 shows the measured spectra from the individual filters after data processing. Each filter output has a transmission peak that closely matches the simulation result with a few nanometers shift.

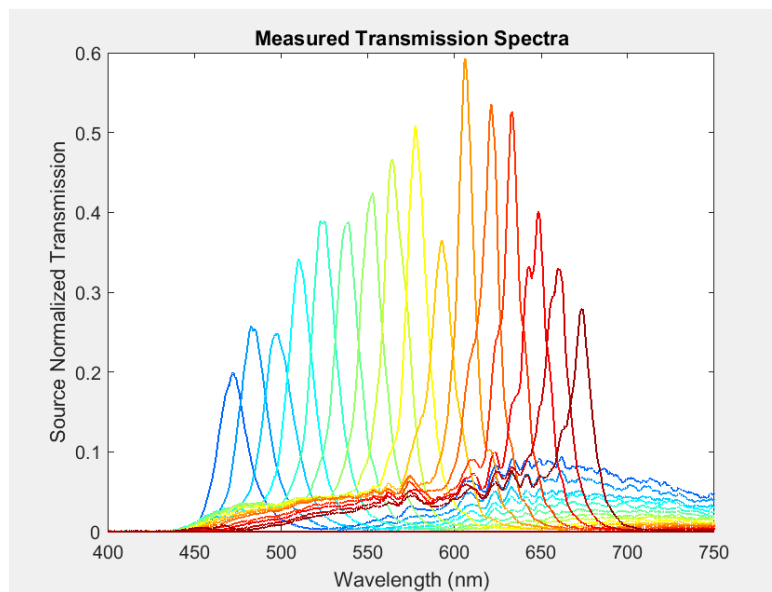


Figure 10: Measured Transmission Spectra of the filter Array

The filters have FWHMs ranging from 14nm to 19nm. The filters on the shorter wavelength side has long tails, whereas the filters on the longer wavelength side shows a secondary peak due to Rayleigh Anomaly effect [22].

#### 4.3 Future Application

As reported in [23], this device was used for high-fidelity visible-light spectroscopy. Signals from color filters were reliably reconstructed combining the filter array with a CMOS imager. Potential future application will be to fabricate an CMOS imager array on top of the plasmonic filter array to achieve on-chip system for signal reconstruction.

#### 5 Conclusion

Aluminum metal grating based plasmonic filters having narrowband transmission peaks and enhanced field distributions were designed for visible light spectroscopy application. An array of 20 filters were fabricated using single step focused ion beam etching on a single device. Each filter has a transmission peak with an average FWHM of 17nm covering the whole visible light range of 400nm to 700nm. The filter outputs closely match the simulation results. Although the filters were characterized using a fiber-based testing setup for this project, after characterization the filters were used in combination with a CMOS imager to demonstrate the potential application for on-chip high-fidelity signal reconstruction system.

## Bibliography

- [1] Gramotnev, Dmitri K., and Sergey I. Bozhevolnyi, "Plasmonics beyond the diffraction limit", *Nature photonics*, vol. 4 no. 2, p. 83, 2010.
- [2] Schuller, Jon A., et al., "Plasmonics for extreme light concentration and manipulation", *Nature materials*, vol. 9, no. 3, pp. 193-204, 2010.
- [3] Pitarke, J. M., et al., "Theory of surface plasmons and surface-plasmon polaritons", *Reports on progress in physics*, vol. 70, no. 1, p. 1, 2006.
- [4] Zayats, Anatoly V., Igor I. Smolyaninov, and Alexei A. Maradudin, "Nano-optics of surface plasmon polaritons", *Physics reports*, vol. 408, no. 3-4, pp. 131-314, 2005.
- [5] Bethe, Hans Albrecht, "Theory of diffraction by small holes", *Physical review*, vol. 66, no. 7-8, pp. 163, 1944.
- [6] Ebbesen, T. W., et al., "Extraordinary optical transmission through sub wavelength hole arrays", *Nature*, vol. 391, pp. 667– 669, 1998.
- [7] Gordon, Reuven, et al., "A new generation of sensors based on extraordinary optical transmission", *Accounts of chemical research*, vol. 41, no. 8, pp. 1049-1057, 2008.
- [8] Do, Yun Seon, et al., "Plasmonic color filter and its fabrication for large-area applications", *Advanced Optical Materials*, vol. 1, no. 2, pp. 133-138, 2013.
- [9] Yokogawa, Sozo, Stanley P. Burgos, and Harry A. Atwater, "Plasmonic color filters for CMOS image sensor applications", *Nano letters*, vol. 12, no. 8, pp. 4349-4354, 2012.
- [10] Kaplan, Alex F., Ting Xu, and L. Jay Guo, "High efficiency resonance-based spectrum filters with tunable transmission bandwidth fabricated using nanoimprint lithography", *Applied Physics Letters*, vol. 99, no. .14, p. 143111, 2011.
- [11] Li, Zhongyang, Serkan Butun, and Koray Aydin, "Large-area, lithography-free super absorbers and color filters at visible frequencies using ultrathin metallic films" *ACS Photonics*, vol. 2, no. 2, pp. 183-188, 2015.
- [12] Gu, Yinghong, et al., "Color generation via subwavelength plasmonic nanostructures", *Nanoscale*, vol. 7, no. 15, pp. 6409-6419, 2015.
- [13] Olson, Jana, et al., "Vivid, full-color aluminum plasmonic pixels", *Proceedings of the national academy of sciences*, vol. 111, no. 40, pp. 14348-14353, 2014.



- [14] Burgos, Stanley P., Sozo Yokogawa, and Harry A. Atwater, "Color imaging via nearest neighbor hole coupling in plasmonic color filters integrated onto a complementary metal-oxide semiconductor image sensor," *ACS nano*, vol. 7, no. 11, pp. 10038-10047.
- [15] Liu, Y. J., et al., "Optically tunable plasmonic color filters", *Applied Physics A*, vol. 107, no. 1, pp. 49-54, 2012.
- [16] Chen, Qin, et al., "CMOS photodetectors integrated with plasmonic color filters", *IEEE Photonics Technology Letters*, vol. 24, no.3, pp. 197-199, 2011.
- [17] Chen, Qin, and David RS Cumming, "High transmission and low color cross-talk plasmonic color filters using triangular-lattice hole arrays in aluminum films", *Optics express*, vol. 18, no. 13, pp. 14056-14062, 2010.
- [18] Inoue, Daisuke, et al., "Polarization independent visible color filter comprising an aluminum film with surface-plasmon enhanced transmission through a subwavelength array of holes", *Applied Physics Letters*, vol. 98, no. 9, pp. 093113, 2011.
- [19] Xu, Ting, et al., "Plasmonic nanoresonators for high-resolution colour filtering and spectral imaging", *Nature communications*, vol. 1, no. 1, pp. 1-5, 2010.
- [20] Knight, Mark W., et al., "Aluminum for plasmonics." *ACS nano*, vol. 8, no. 1, pp. 834-840, 2014.
- [21] Moharam, M. G., and T. K. Gaylord, "Rigorous coupled-wave analysis of planar-grating diffraction." *JOSA*, vol. 71, no. 7, pp. 811-818, 1981.
- [22] Chong, Xinyuan, et al. "On-chip near-infrared spectroscopy of CO<sub>2</sub> using high resolution plasmonic filter array", *Applied Physics Letters*, vol. 108, no. 22, pp. 221106, 2016.
- [23] Shakya, Jyotindra R., Farzana H. Shashi, and Alan X. Wang, "High-Fidelity Visible-Light Spectroscopy using Aluminum Plasmonic Grating Filter Array", *Laser Science*. Optical Society of America, 2019.